ISSN 1070-3632, Russian Journal of General Chemistry, 2007, Vol. 77, No. 4, pp. 629–640. © Pleiades Publishing, Ltd., 2007.
Original Russian Text © N.Sh. Lebedeva, N.A. Pavlycheva, A.I. V'yugin, 2007, published in Zhurnal Obshchei Khimii, 2007, Vol. 77, No. 4, pp. 674–686.

Kinetics of Thermal Oxidative Decomposition of Zinc Porphyrin and Phthalocyanine Complexes

N. Sh. Lebedeva, N. A. Pavlycheva, and A. I. V'yugin

Institute of Solution Chemistry, Russian Academy of Sciences,
ul. Akademicheskaya 1, Ivanovo, 153045 Russia
e-mail: nsl@isc-ras.ru

Received June 5, 2006

Abstract — Thermal oxidative decomposition of certain zinc porphyrin and phthalocyanine complexes was studied using an installation for thermal analysis, and kinetic parameters of the thermal oxidation of these compounds were determined. The introduction of peripheral alkyl substituents into porphyrin molecules enhances the macroring stability with respect to the thermal oxidation. In cases of benzoporphyrins and phthalocyanines, this effect is leveled off because of spatial remoteness of the substituent from the reactive center of the macroring. The substances studied decompose in several steps; the initial step corresponds to the oxidation of peripheral substituents of the macroring. For the majority of the substances studied, the order of the thermal oxidation reaction is 1, and the main step controlling the thermal oxidation process is diffusion.
DOI: 10.1134/S1070363207040226

Macroheterocyclic compounds, such as metal porphyrins and phthalocyanines, have unique physical and chemical properties. Semiconducting, optical, catalytic, and other practically useful properties of these macrocyclic substances are well known. New possibilities of the functional use of porphyrin and phthalocyanine compounds have beem revealed recently, e.g., their capability for self-organization (self-assembly) can form a basis for nanotechnologies [1]. Thin films, from nanometers to micrometers in thickness, are prepared by sublimation of macroheterocycles [1] or by Langmuir–Blodgett technique [2]. In both cases, a substance or films are subjected to thermal treatment. In some cases, the thermal treatment can lead to a polymorphous transition [3, 4], to the formation of polymeric structures [5, 6], or to decomposition of the macroring [5–7]. Therefore, there is a need for the information concerning the thermal stability of macroheterocyclic substances and the effects of peripheral functional substituents and the nature of the macroring itself on the resistance of macroheterocycles to thermal oxidation.

As a rule, published information on the thermal stability is limited, and we failed to find in the literature any kinetic characteristics of the thermal oxidation of metal porphyrins and phthalocyanines. Therefore, the aim of this study was to examine the thermochemistry of a wide set of zinc complexes of porphyrins and phthalocyanines and to determine the kinetic parameters of their thermal oxidation.

To estimate the effects of the macroheteroring nature and of the symmetry and nature of peripheral functional substituents on the resistance of macroheterocyclic substances to thermal oxidation, we chose the following subjects of the study: zinc(II) tetraphenylporphyrin (ZnTPhP) (**I**), zinc(II) tetra-*tert*-butyltetraphenylporphyrin [Zn(*t*-Bu)$_4$TPhP] (**II**), zinc(II) hematoporphyrin **IX** (ZnHP) (**III**), zinc(II) deuteroporphyrin **IX** (ZnDP) (**IV**), zinc(II) protoporphyrin **IX** (ZnPP) (**V**), zinc(II) tetrabenzoporphyrin (ZnTBP) (**VI**), zinc(II) tetra-*tert*-butyltetrabenzoporphyrin [Zn(*t*-Bu)$_4$TBP] (**VII**), zinc(II) tetraphenyltetrabenzoporphyrin (ZnTPhTBP) (**VIII**), zinc(II) phthalocyanine (ZnPc) (**IX**), and zinc(II) tetra-*tert*-butylphthalocyanine [Zn(*t*-Bu)$_4$Pc] (**X**).

Typical thermograms of the substances under study are shown in Figs. 1–10. The data obtained indicate that the metal complexes of the macroheterocyclic substances under study are rather stable against thermal oxidative decomposition. They start to decompose at temperatures exceeding 536 K, and the decomposition process is complicated, as demonstrated by the presence of several, sometimes ill-resolved, maxima and minima in the DTA and DTG curves. It is noted in the literature [8] that the thermal oxidation of macroheterocycles of the porphyrin and phthalocyanine series occurs in several steps involving the oxidation of peripheral substituents, the rupture of a macroheterocycle, and the oxidation to higher oxides.

Data on the thermal oxidation of zinc porphyrin and phthalocyanine complexes are presented in

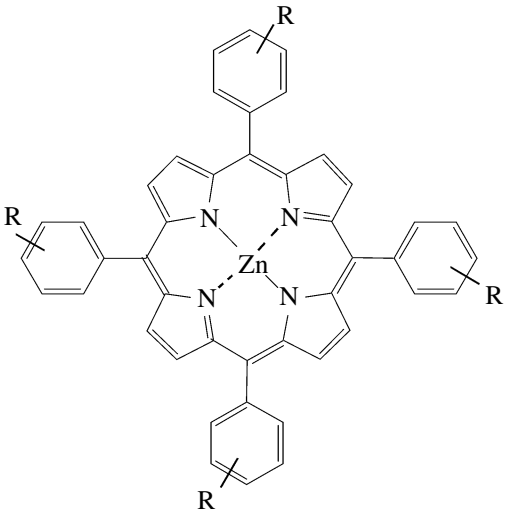

I, II

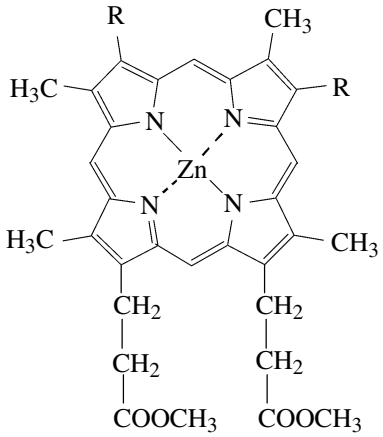

III–V

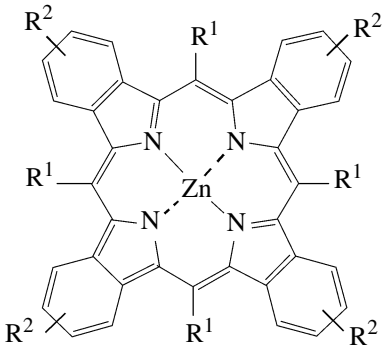

VI–VIII

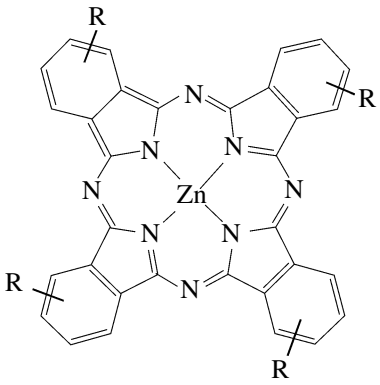

IX, X

R = H (**I, IV, IX**), C_4H_9 (**II, X**); $CH(OCH)_3CH_3$ (**III**), $CH_2{=}CH_2$ (**V**); $R^1 = R^2 = H$ (**VI**); $R^1 = H$, $R^2 = C_4H_9$ (**VII**); $R^1 = C_6H_5$; $R^2 = H$ (**VIII**).

Table 1. Thermal oxidative decomposition of metal complexes of macroheterocyclic compounds

Process	Temperature range, K	Residue, wt%	
		calculated	found
ZnHP → ZnO	536–820	11.33	10.71
ZnDP → ZnO	609–820	13.52	13.48
ZnPP → ZnO	621–807	12.44	12.03
ZnTPhP → ZnO	623–832	12.00	11.89
Zn(*t*-Bu)$_4$TPhP → ZnO	667–903	9.02	8.62
ZnTPhTBP → ZnO	633–838	9.27	8.76
ZnTBP → ZnO	630–800	14.18	13.90
Zn(*t*-Bu)$_4$TBP → ZnO	595–857	10.15	10.14
ZnPc → ZnO	750–857	14.17	13.88
Zn(*t*-Bu)$_4$Pc → ZnO	671–861	10.14	10.05

Table 1. For convenience of discussing and comparing the kinetic parameters of the thermal oxidation of the macroheterocycles, the processes under study were divided into separate steps characteristic for each macrocycle. The corresponding temperature ranges and kinetic characteristics are given in Tables 2 and 3.

The data obtained show that the kinetic characteristics of the processes under study, determined using the Coates–Redfern and Sestak–Berggren procedures, practically coincide, whereas the activation energies estimated from the DTG curve differ by 2–9% (steps I and II) or by 20–100% (step III). Such a high error seems to be caused by high rate of the process and is a limitation of the approach to estimating E_a suggested in [9]. Therefore, the averaged values of the kinetic parameters for all the zinc porphyrin and phthalocyanine complexes were determined taking into account the values calculated by the Coates–Redfern and Sestak–Berggren procedures (Table 4).

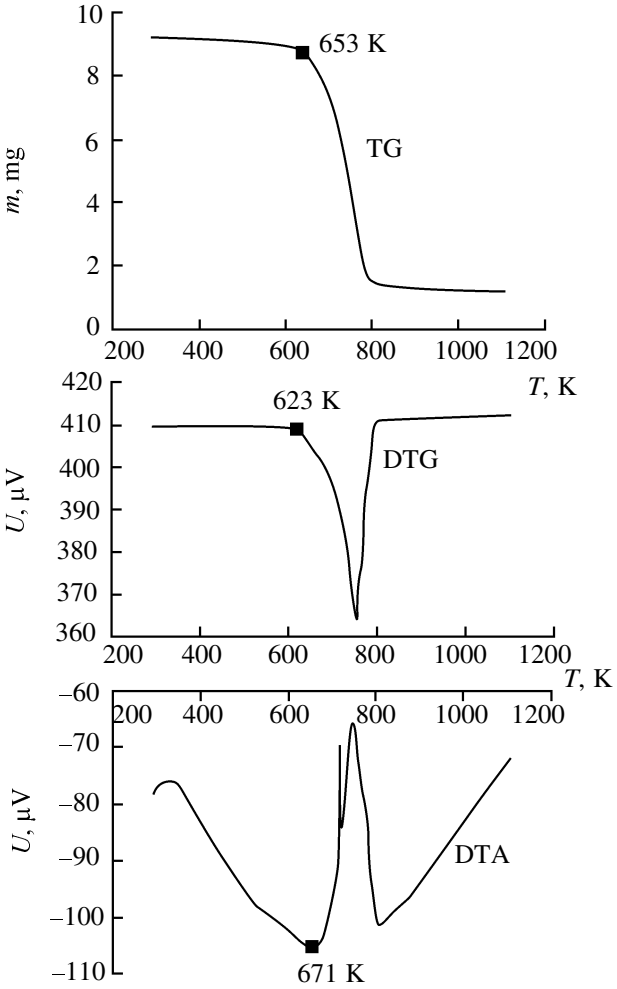

Fig. 1. Thermogram of ZnTPhP.

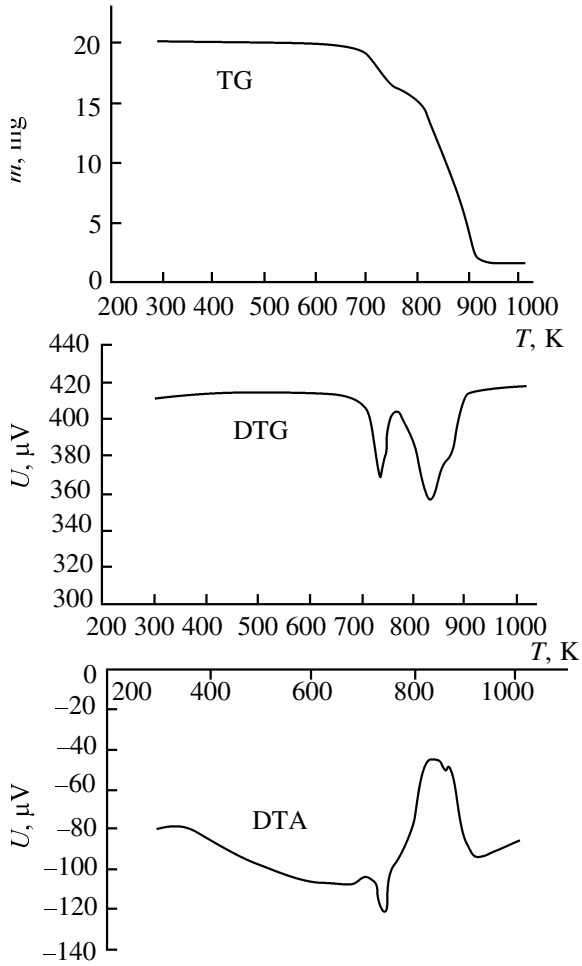

Fig. 2. Thermogram of Zn(*t*-Bu)$_4$TPhP.

Let us consider the data on the thermal oxidative decomposition of ZnTPhP (Fig. 1). The process is rather intense and is accompanied by an appreciable exo effect in the DTA curve. There are various procedures for evaluating the decomposition temperatures of macroheterocycles. For example, the decomposition temperature of ZnTPhP determined in the minimum point of the DTA curve is 671 K [7], whereas analysis of the TG curve gives the decomposition temperature of ZnTPhP of 653 K [10]. These temperatures are marked in the thermogram (Fig. 1). In fact, the temperatures of 671 and 653 K correspond to certain changes in the run of the curves under consideration; however, in our opinion, the decomposition temperature of a macroheterocycle can be estimated more accurately from the DTG curve, as, unlike the DTA curve, it shows no lag and, being the first derivative of TG, will reflect more clearly a change in the TG curve slope. Judging from the DTG curve, the decomposition temperature of ZnTPhP is 623 K, and the reaction order is 1 (Table 3), which is typical for the thermal oxidation of crystalline substances [11]. The reaction order n 0.8–1 suggests that in this case diffusion is the limiting stage [12].

The thermograms of alkyl-substituted zinc(II) tetraphenylporphyrin Zn(*t*-Bu)$_4$TPhP are essentially

Table 2. Temperature ranges (K) of steps I–III of thermal oxidative decomposition of metal complexes of macroheterocyclic compounds

Compound	I	II	III
ZnHP	536–650	650–725	725–820
ZnDP	609–699	722–820	
ZnPP	621–690	690–807	
ZnTPhP			623–832
Zn(*t*-Bu)$_4$TPhP		667–805	805–903
ZnTPhTBP	633–740	740–786	786–838
ZnTBP			630–800
Zn(*t*-Bu)$_4$TBP		595–713	762–857
ZnPc			750–857
Zn(*t*-Bu)$_4$Pc		671–729	742–861

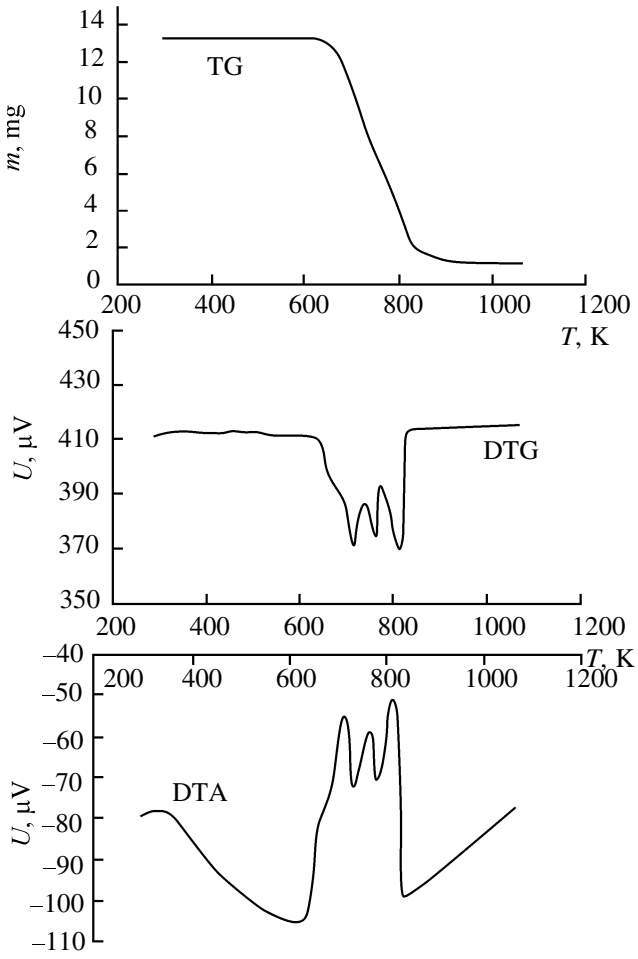

Fig. 3. Thermogram of ZnTPhTBP.

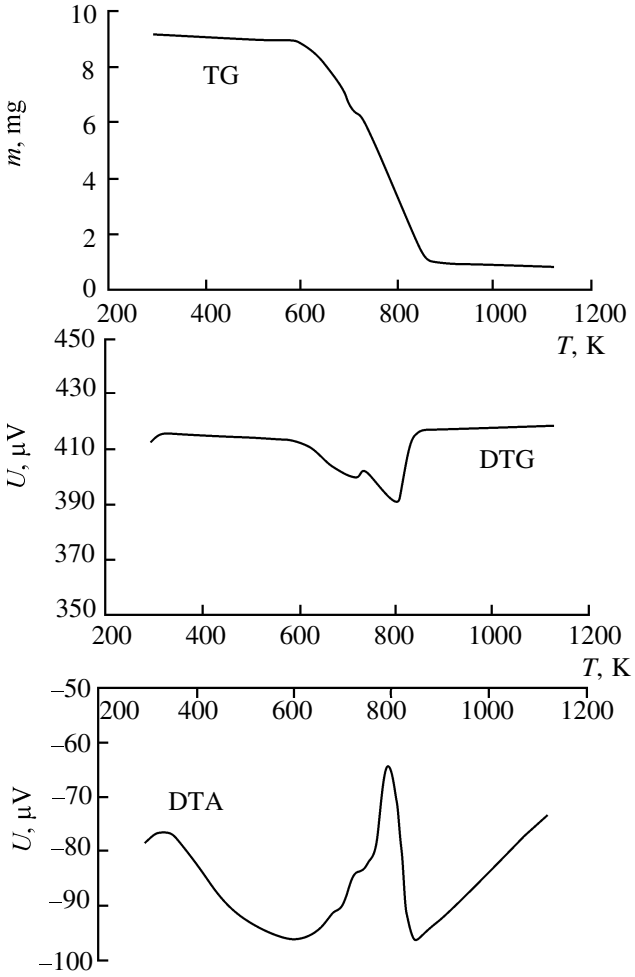

Fig. 4. Thermogram of Zn(*t*-Bu)$_4$TBP.

different. Two clear peaks are detected in the DTG curve at high temperatures (above 600 K) (Fig. 2). The temperature of Zn(*t*-Bu)$_4$TPhP decomposition is higher than that of ZnTPhP. Probably, alkyl substituents exerting a positive inductive effect stabilize a macroheterocycle by enhancing the strength of the bond of the central metal ion with the porphyrin macroring. A similar conclusion on the effect of alkyl substitution in metal porphyrins was made in [13] when studying the standard enthalpies of sublimation

Table 3. Kinetic parameters of the reaction of thermal oxidation of macroheterocyclic substances

Compound	Step no.	E, kJ mol^{-1}	ln A	n	r^2	$F(\alpha)$	Model	Calculation procedure
ZnTPhP	III	230.28			0.985			DTG
		196.08		1	0.985			[a]
		185.72	33.74	1	0.975	$1 - \alpha$	F1	[b]
Zn(*t*-Bu)$_4$TPhP	II	283.03			0.985			DTG
		231.72			0.991			[a]
		232.57	41.32	1	0.968	$1 - \alpha$	F1	[b]
	III	449.00			0.951			DTG
		357.46		2	0.987			[a]
		360.56	54.53	2	0.951	$(1 - \alpha)^2$	F2	[b]

Table 3. (Contd.)

Compound	Step no.	E, kJ mol^{-1}	ln A	n	r^2	$F(\alpha)$	Model	Calculation procedure
ZnTPhTBP	I	193.11			0.854			DTG
		209.41		1	0.931			[a]
		188.92	35.17	1	0.907	1 – α	F1	[b]
	II	565.18			0.972			DTG
		585.98		1	0.953			[a]
		590.14	95.63	1	0.940	1 – α	F1	[b]
ZnTPhTBP	III	691.75			0.964			DTG
		645.72		1	0.922			[a]
		646.35	95.55		0.767		D2	[b]
ZnTBP	III	251.80			0.982			DTG
		206.68		1	0.985			[a]
		203.15	32.98	1	0.973	1 – α	F1	[b]
Zn(*t*-Bu)$_4$TBP	II	143.31			0.985			DTG
		141.24		1	0.996			[a]
		140.55	28.19	1	0.994	1 – α	F1	[b]
	III	421.51			0.981			DTG
		350.10		1	0.996			[a]
		342.31	54.02	1	0.978	1 – α	F1	[b]
ZnHP	I	93.14			0.986			DTG
		87.06		1	0.983			[a]
		84.73	19.57	1	0.896	1 – α	F1	[b]
	II	155.55			0.981			DTG
		156.11		1	0.998			[a]
		153.52	29.80	1	0.968	1 – α	F1	[b]
	III	465.68			0.997			DTG
		266.95		1	0.968			[a]
		251.21	43.15	1	0.931	1 – α	F1	[b]
ZnDP	II	179.95			0.989			DTG
		155.83		1	0.993			[a]
		152.25	30.39	1	0.848	1 – α	F1	[b]
	III	486.54			0.923			DTG
		280.06		1	0.979			[a]
		281.08	46.50	1	0.944	1 – α	F1	[b]
ZnPP	II	183.48			0.968			DTG
		188.69		1	0.993			[a]
		193.41	37.50	1	0.993	1 – α	F1	[b]
	III	654.49			0.995			DTG
		403.19		1	0.951			[a]
		401.47	67.84	1	0.969	1 – α	F1	[b]
ZnPc	III	432.32			0.993			DTG
		398.08		1	0.957			[a]
		416.54	75.66	1	0.972	1 – α	F1	[b]
Zn(*t*-Bu)$_4$Pc	II	654.01			0.938			DTG
		391.67		1	0.991			[a]
		389.77	71.47	1	0.938	1 – α	F1	[b]
	III	698.45			0.971			DTG
		326.15		1	0.992			[a]
		322.176	52.49	1	0.946	1 – α	F1	[b]

[a] Coates–Redfern procedure. [b] Sestak–Berggren procedure.

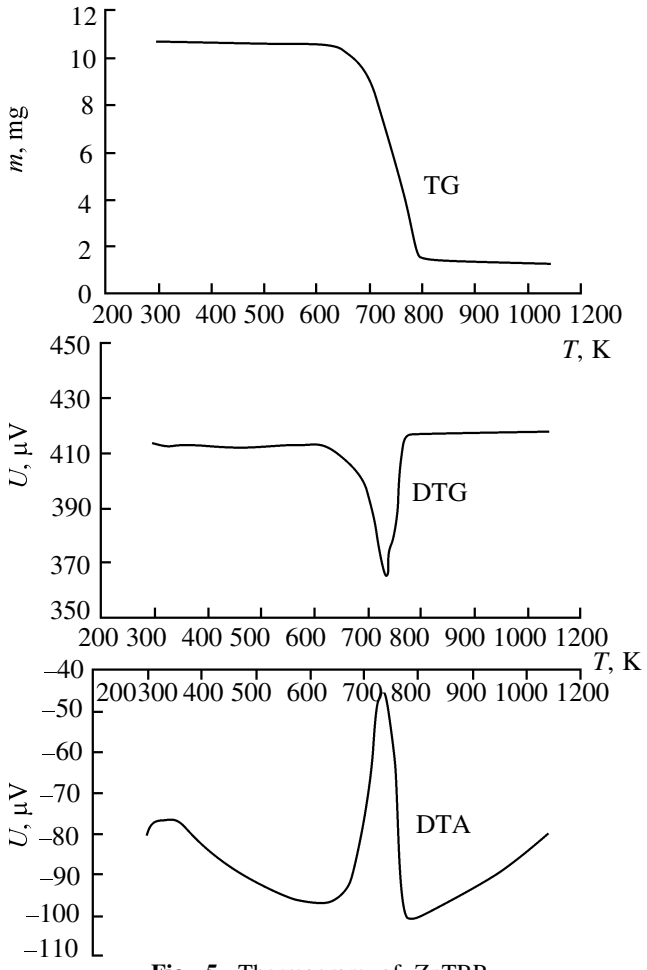

Fig. 5. Thermogram of ZnTBP.

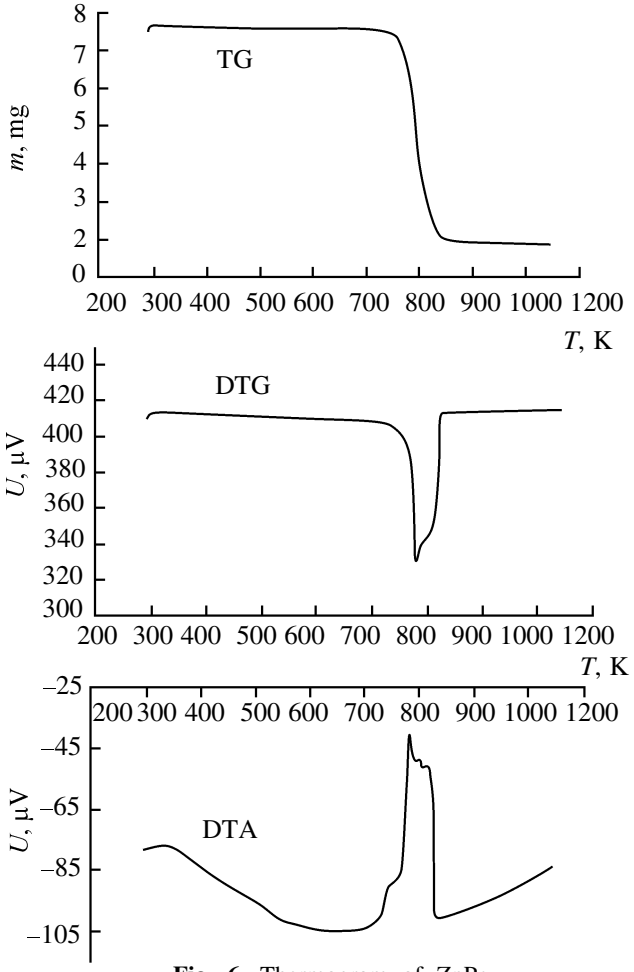

Fig. 6. Thermogram of ZnPc.

and formation of cobalt(II) tetraphenylporphyrin derivatives. The decomposition of Zn(*t*-Bu)$_4$TPhP starts at 667 K and occurs with a considerable weight loss up to a temperature of 805 K. The DTA curve in this segment is complicated, a slight exo effect recorded in the temperature range 711–725 K "breaks" and gives way to an appreciable endo effect. The DTG curve reflects the difference in temperatures of a sub-

Table 4. Averaged kinetic parameters of steps I–III of thermal oxidative decomposition of metal complexes of macroheterocyclic compounds

Compound	I		II		III	
	E_a, kJ mol^{-1}	ln A	E_a, kJ mol^{-1}	ln A	E_a, kJ mol^{-1}	ln A
ZnHP	88.31	19.57	155.06	29.80	259.08	43.15
ZnDP			154.04	30.39	280.57	46.50
ZnPP			188.45	37.50	402.33	67.84
ZnTPhP					190.90	33.74
Zn(*t*-Bu)$_4$TPhP [a]			231.65	41.32	359.01	54.01
ZnTPhTBP [b]	195.75	35.17	588.14	95.63	646.04	95.55
ZnTBP					204.92	32.98
Zn(*t*-Bu)$_4$TBP			141.70	28.19	346.21	54.02
ZnPc					415.65	75.66
Zn(*t*-Bu)$_4$Pc			390.72	71.47	324.17	52.49

[a] Limiting step F2. [b] Limiting step D2.

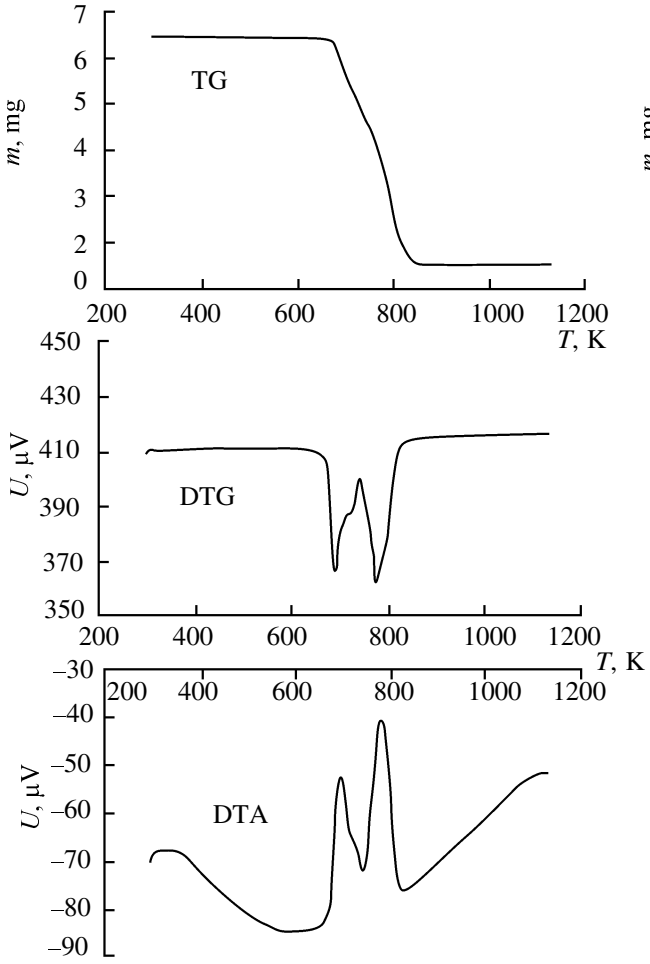

Fig. 7. Thermogram of Zn(*t*-Bu)$_4$Pc.

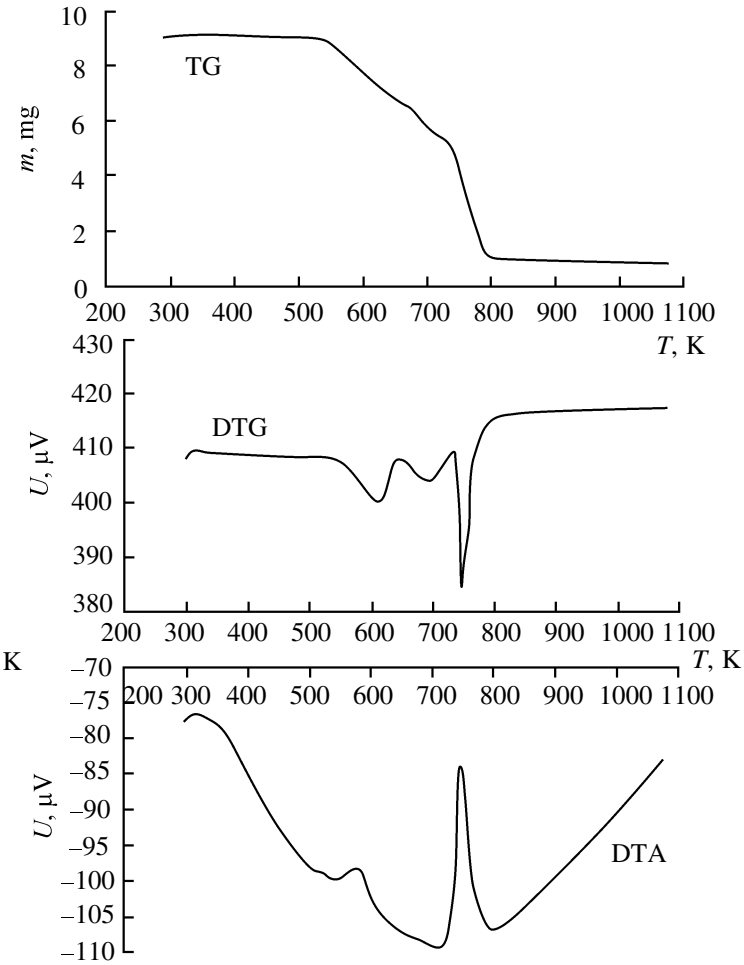

Fig. 8. Thermogram of ZnHP.

stance under study and a reference (Al_2O_3); therefore, it can be expected that in the case of very intense removal of gaseous products of Zn(*t*-Bu)$_4$TPhP pyrolysis the temperature of the sample under study will decrease, despite the heat release in the oxidation. In such a case, a sharp peak should be recorded in the DTG curve. However, judging from the deviation of the DTG signal from the baseline of the DTG curve (Fig. 2), the rate of removal of gaseous products of the Zn(*t*-Bu)$_4$TPhP thermal oxidation is low and does not affect the shape of the DTA curve. Therefore, we assumed that the macrocycle is dealkylated in this step to form polymeric porphyrin structures. This assumption is supported by the calculations based on TG: four *tert*-butyl groups make up 25% of the molecule weight, whereas the experimental weight loss in this step is 24.8%. The formation of polymeric structures in step II is also confirmed by the kinetic characteristics of step III, corresponding to the macrocycle cleavage and oxidation to higher oxides, which is especially noticeable when comparing the temperatures and activation energies of steps III of Zn(*t*-Bu)$_4$TPhP and ZnTPhP oxidation, which are considerably higher in the case of Zn(*t*-Bu)$_4$TPhP or, more precisely, of its pyrolysis products. Another specific feature distinguishing the thermal oxidation of Zn(*t*-Bu)$_4$TPhP from that of all the other macroheterocycles studied is its compliance with the model of a second-order heterogeneous reaction mechanism (F2), whereas the thermal oxidative decomposition of the other macroheterocycles obeys the mathematical model of the first-order reaction (F1).

The expansion of an aromatic system due to the annelation of benzene rings with tetrapyrrole fragments of a macroheteroring in going from ZnTPhP to ZnTPhTBP enhances the resistance of this macrocycle to thermal oxidation (Fig. 3). The pyrolysis of ZnTPhTBP occurs in three steps. It was assumed [8] that four phenyl group are removed in the first step. However, our calculations of the weight loss have not confirmed this assumption, as the percentage of four

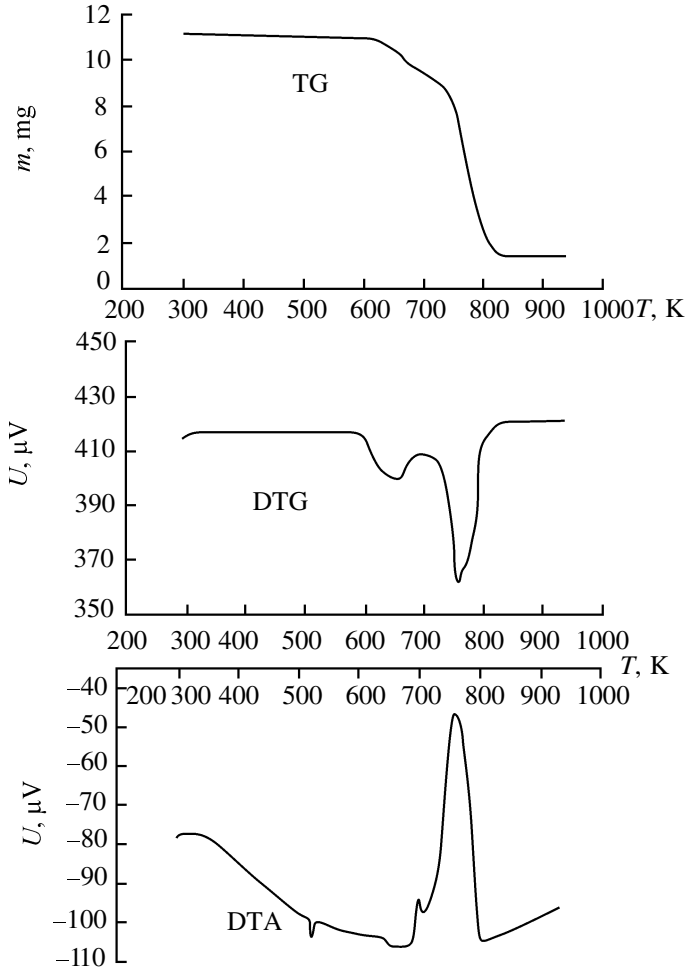

Fig. 9. Thermogram of ZnDP.

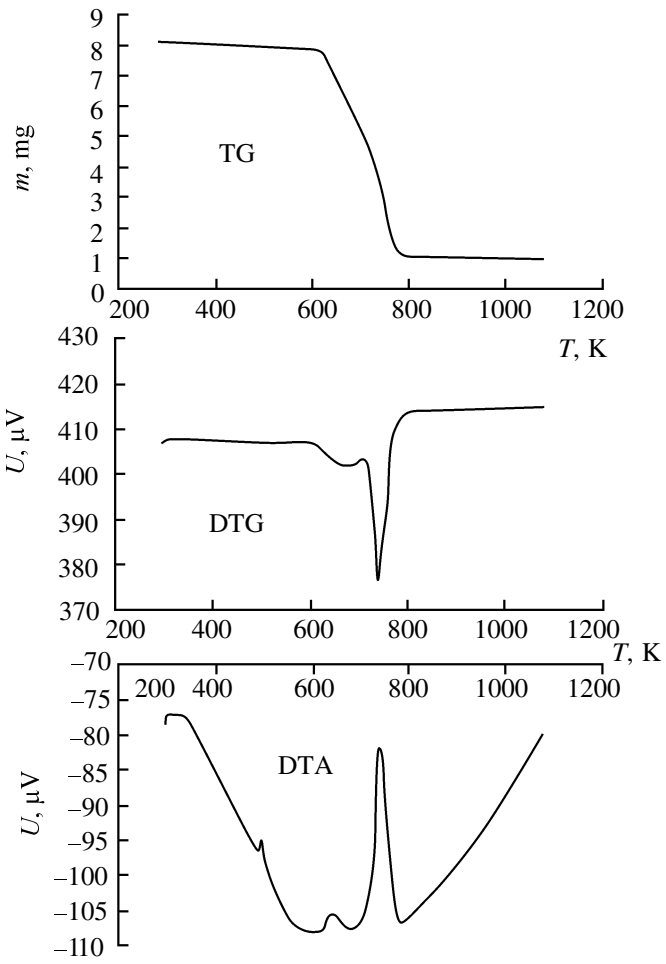

Fig. 10. Thermogram of ZnPP.

phenyl groups in a ZnTPhTBP molecule is 35.07%, whereas the recorded weight loss of the sample in the first step is 42.76%. The pyrolysis of ZnTPhTBP starts at 633 K, its activation energy being slightly higher than the activation energy of ZnTPhP thermal oxidation. Apparently, the reason for increasing stability of the ZnTPhTBP macroheterocycle is strengthening of the macrocyclic π-electron shielding effect owing to expansion of the aromatic system upon annelation of aromatic rings (pyrrole and benzene).

A comparison of the kinetic parameters of the ZnTPhTBP and ZnTBP thermal oxidation allows estimation of the effect of phenyl substituents in *meso*-positions of the macroring on the resistance of macromolecules to thermal oxidation. Although these macroheterocycles have close decomposition temperatures, the activation energy of ZnTPhTBP thermal oxidation is approximately 1.3 times higher than that calculated for ZnTBP. Phenyl groups are characterized by an electron-donor effect; therefore, their introduction into a porphyrin molecule increases the electron density on nitrogen atoms of the reactive center, thus increasing the strength of the bond between the central metal ion and the macrocyclic ligand and hence the resistance of the complex to the thermal oxidation. An essential role of the central metal ion in thermal oxidation processes is proved by the data of [7, 8], where it was shown that replacement of the central metal ion in metal porphyrins, e.g., of Zn^{2+} by Co^{2+} in tetraphenylporphyrin, decreases the macrocycle stability by more than 100 K. Our results and published data suggest that axial coordination of molecular oxygen is one of the initial steps of thermal oxidative decomposition of metal complexes of macroheterocyclic substances. Except for an inductive effect, phenyl groups can exhibit $+C$ electronic effect. As numerous calculations and X-ray structural data show, in the ZnTPhP molecule the conjugation effect of phenyl substituents is negligible, as benzene rings, according to the data of various authors, are located at an angle of 20°–40° to the macroring plane.

However, it is possible that in the case of ZnTPhTBP the annelated benzene rings will give rise to steric hindrances to the turning of phenyl substituents. It should also be taken into account that the conformation mobility of molecules in the crystalline state is essentially limited in comparison with the gas phase. The final step of the ZnTPhTBP thermal oxidation is described by the two-dimensional diffusion (D2) equation.

Let us compare the results of the thermochemical study of ZnTBP and Zn(*t*-Bu)$_4$TBP. Introduction of peripheral *tert*-butyl groups into a ZnTBP molecule, in contrast to ZnTPhP, does not enhance the stability of the macrocycle (Tables 1, 2). In this case, probably, alkyl groups are located too far from the porphyrin reactive center and, as the electronic effect practically completely fades out even in a chain of four hydrocarbon groups [14], their influence on the $Zn^{2+} \leftarrow$ porphyrin bond is reduced practically to zero. However, relatively bulky peripheral substituents will distort the macroring planarity and cause a decrease in the macrocyclic effect of π-electron shielding. The thermal oxidation of Zn(*t*-Bu)$_4$TBP is a two-step process (Fig. 4). By analogy with Zn(*t*-Bu)$_4$TPhP, in the first step, probably, peripheral substituents of the macroring are mostly oxidized and removed, which agrees with the calculated weight loss of 28.08% (the percentage of four butyl groups in a Zn(*t*-Bu)$_4$TBP molecule is 28.43%). It is remarkable that the temperature and the activation energy of the thermal oxidation of peripheral *tert*-butyl groups in Zn(*t*-Bu)$_4$·TPhP molecules are much higher than in Zn(*t*-Bu)$_4$TBP molecules. Furthermore, the oxidation of peripheral *tert*-butyl substituents in a Zn(*t*-Bu)$_4$TBP molecule is accompanied by only slight exo effect in the DTA curve. The activation energy in the final stage of Zn(*t*-Bu)$_4$TBP thermal oxidation is close to the analogous characteristic for Zn(*t*-Bu)$_4$TPhP, but the limiting step is diffusion (F1).

The replacement of methine bridges by *meso*-N atoms in going from ZnTBP (**VI**) (Fig. 5) to ZnPc (**IX**) (Fig. 6) increases the temperature limit of the macrocycle resistance to thermal oxidation by more than 100 K, with the activation energy necessary for ZnPc pyrolysis increasing by a factor of three. It is known that the introduction of nitrogen atoms in *meso*-positions enhances the macroring aromacity; hence, the macrocyclic effect of π-electron shielding increases. For the same reasons, alkyl-substituted Zn(*t*-Bu)$_4$Pc is more resistant to thermal oxidation than Zn(*t*-Bu)$_4$TPhP.

The comparison of kinetic characteristics of ZnPc and Zn(*t*-Bu)$_4$Pc suggests that in the temperature range 671–729 K *tert*-butyl substituents are probably oxidized, as is the case with zinc(II) porphyrins, as indicated by the 28.04% weight loss (TG curve, Fig. 7), which practically coincides with the weight fraction (28.42%) of four *tert*-butyl substituents in a Zn(*t*-Bu)$_4$Pc molecule. The introduction of *tert*-butyl substituents into a molecule of zinc(II) phthalocyanine, as is also the case with zinc(II) tetrabenzoporphyrin, does not promote stabilization of a macromolecule, which is probably caused by the same reasons as in the case of Zn(*t*-Bu)$_4$TBP, namely, by spatial remoteness of peripheral substituents from the macrocycle reactive center.

Let us consider the thermal oxidation of zinc complexes of protogroup porphyrins. In contrast to symmetrically substituted synthetic porphyrins, natural porphyrins are characterized by dissimilar unsymmetrical peripheral substitution, which strongly affects their physical and chemical properties, including the resistance to the thermal oxidation (Tables 1–3). The thermograms of the processes under study for natural zinc(II) porphyrins are very similar to the thermograms obtained for synthetic zinc(II) porphyrins. The processes under study include several stages accompanied by exo effects in the DTA curve. In the case of ZnHP (Fig. 8), three main steps are clearly seen, whereas two steps take place for ZnDP (Fig. 9) and ZnPP (Fig. 10). It should also be noted that a small endo effect at 530 K, accompanied by no weight loss, is present in the DTA curve of ZnDP (Fig. 9). Most probably, conformational changes occur at this temperature, as melting is not characteristic of metal porphyrin complexes. Melting was observed only for metal-free analogs, in particular, for deuteroporphyrin **IX** which melts at 492 K [15]. Heating of ZnPP to 494 K also probably results in conformation changes, as a small exo effect accompanied by no weight loss is detected at this temperature in the DTA curve, whereas no second-kind transitions were found for ZnHP. In a ZnHP molecule, there are four oxygen-containing substituents, in contrast to the other natural zinc(II) porphyrins represented by dimethyl esters. It is possible that the absence of conformation changes in the case of ZnHP is caused by stabilization of the macroring structure due to formation of hydrogen bonds between the neighboring ZnHP molecules.

Natural metal porphyrins have lower decomposition temperatures than synthetic macroheterocycles; thus, the asymmetry of the peripheral substitution negatively affects the macrocycle thermal stability. The temperatures of the onset of the thermal oxidative decomposition of zinc(II) porphyrins and the activation energies of the processes increase in the following order: ZnHP < ZnDP < ZnPP. Zinc(II) porphyrins

under study differ only in the nature of substituents in positions 2 and 4; therefore, the observed differences can be associated only with the effect of substituents. Hydrogen in ZnDP has a zero electronic effect. As shown previously [16], in hematoporphyrin the electronic effect of the complex substituent $CH(OCH_3)CH_3$ is determined by the sum of the electronic effects of the CH_3O and $CH_3CH=$ groups, and $-I(CH_3O) > +I(CH_3CH=)$. The CH_3O group exhibiting $+C$ and $-I$ effects can exhibit only the $-I$ effect in the composition of this substituent, because the CH group acts as insulator preventing the conjugation of the p_z electrons of the oxygen atom with the π system of the porphyrin macroring. The negative inductive effect of the $CH(OCH_3)CH_3$ substituents will reduce the electron density on the central nitrogen atoms of the reaction center of the porphyrin molecule, causing weakening of the Zn^{2+}–porphyrin bond. The opposite effect on the macrocycle stability and the strength of the Zn^{2+}–porphyrin bonds will be exerted by the vinyl group $CH=CH_2$, which, as known, exhibits $+I$ and $+C$ electronic effects in porphyrins.

Let us consider step-by-step the thermal oxidation of ZnHP. The weight loss of the sample under study in the first and second steps is 24.56 and 16.15%, which agrees with the percent content of peripheral substituents in positions 6, 7 (24.22%) and 2, 4 (16.43%) of the macroring. It was logical to expect that the thermal oxidative decomposition of ZnDP and ZnPP would also start with the oxidation of peripheral oxygen-containing substituents. However, the weight percentage of two $(CH_2)COOCH_3$ groups in ZnDP and ZnPP (28.90 and 26.60%) disagrees with the weight loss determined from the TG curve. The weight loss in step II of the ZnDP and ZnPP pyrolysis is 16.56 and 19.77%, respectively. Thus, a study of the natural metal porphyrins chosen as examples shows that peripheral substituents of various nature not only significantly affect the macroheterocycle stability, but also determine the thermal oxidation mechanism.

Thus, our research showed that the simplified procedure for calculating the activation energy, suggested in [9], gives overestimated kinetic parameters in the case of a high rate of the process under study. We found that the kinetic and thermal stability of zinc(II) porphyrins and zinc(II) phthalocyanines increases in the following series of macroheterocycles:

ZnHP < Zn(*t*-Bu)$_4$TBP < ZnDP < ZnPP < ZnTPhP < ZnTBP = ZnTPhTBP < Zn(*t*-Bu)$_4$TPhP < Zn(*t*-Bu)$_4$Pc < ZnPc.

EXPERIMENTAL

The electronic absorption spectra were recorded on a Specord M400 (Germany) double-beam spectrophotometer in the spectral range from 300 to 800 nm, using 10-mm quartz cells.

All the substances under study were synthesized by standard procedures [17, 18]. In all cases, except for zinc(II) phthalocyanine, macroheterocyclic substances were purified by chromatography on Al_2O_3 (Brockmann grade II) using benzene, chloroform, pyridine, and their mixtures as eluents. Zinc(II) phthalocyanine was purified by vacuum sublimation. Before studying, all the substances were dried in a vacuum to remove adsorbed molecules of solvents and water. The purity of the products was checked by the electronic absorption spectra, which showed good agreement with the published data [17, 18]. The purity of zinc(II) phthalocyanine was checked only by its elemental analysis because of its insolubility in organic solvents (Table 5).

Table 5. Elemental analysis of zinc complexes of macroheterocycles

Complex	Found, %			Formula	Calculated, %		
	C	H	N		C	H	N
ZnTPhP	77.53	4.13	8.17	$ZnC_{44}H_{28}N_4$	77.92	4.16	8.27
Zn(*t*-Bu)$_4$TPhP	80.54	6.74	6.19	$ZnC_{60}H_{60}N_4$	79.83	6.71	6.21
ZnHP	64.33	7.91	6.19	$ZnC_{38}H_{44}N_4O_6$	63.53	6.18	7.81
ZnDP	63.31	5.25	9.36	$ZnC_{32}H_{32}N_4O_4$	63.82	5.36	9.31
ZnPP	65.68	5.56	8.54	$ZnC_{36}H_{38}N_4O_4$	65.91	5.84	8.54
ZnTBP	75.99	3.53	9.64	$ZnC_{36}H_{20}N_4$	75.32	3.51	9.77
Zn(*t*-Bu)$_4$TBP	79.39	6.60	7.03	$ZnC_{52}H_{52}N_4$	78.21	6.57	7.02
ZnTPhTBP	81.40	4.11	6.39	$ZnC_{60}H_{36}N_4$	82.03	4.13	6.38
ZnPc	67.35	2.82	19.07	$ZnC_{32}H_{16}N_8$	66.49	2.79	19.40
Zn(*t*-Bu)$_4$Pc	72.25	9.97	14.02	$ZnC_{48}H_{48}N_8$	71.84	6.03	13.97

The thermal oxidative decomposition of crystalline samples of macroheterocyclic compounds was studied in air at a heating rate of 5 deg min^{-1} on an installation for thermal analysis, whose metrological and certification characteristics have been described in detail in [19].

The C, H, N analysis was performed on a CHNS-O Analyzer Flash TF 1112 Series device.

Mathematical treatment of data. All possible approaches to the calculation of kinetic parameters of reactions are based on Arrhenius equation (1) reflecting the temperature dependence of the reaction rate constant:

$$k = Ae^{-E/RT}. \quad (1)$$

To obtain more reliable results, the calculations in this study were carried out by three independent procedures [9, 20, 21]. The first two procedures are the most frequently used and well known. They are based on Eq. (2) (ω is weight loss).

$$\left(\frac{m_0}{\omega_\infty}\right)^{1-n} \int_0^{\omega} (\omega_\infty - \omega)^{-n} d\omega = \frac{A}{\varphi} \int_{T_1}^{T_2} e^{-E/R} dT. \quad (2)$$

The right part of the equation can be solved by various methods. The solution of the equation in the final form is an infinite series in which only the first two terms are commonly taken into account. This technique was used by Coates, Redfern, et al. [21].

For reactions with unknown order, Coates and Redfern [21] obtained expression (3).

$$\log \frac{(1-\alpha)^{1-n}}{T^2(1-n)} = \log \frac{AR}{aE}\left(1 - \frac{2RT}{E}\right) - \frac{E}{2.3RT}. \quad (3)$$

Here α is the sample fraction that decomposed in time t, and a is the heating rate. The dependence of

$$\log \frac{(1-\alpha)^{1-n}}{T^2(1-n)}$$

on $1/T$ at correct choice of n or of $\log[-\ln(1-\alpha)]/T^2$ on $1/T$ at $n = 1$ is a straight line with a slope defined by the quantity $-E/2.3R$.

A more informative approach suggested by Sestak and Berggren [20] makes it possible to calculate the kinetic parameters and to find the limiting step of a thermal oxidation process.

For this purpose, Eqs. (4) and (5) are used.

$$d\alpha/dt = kf(\alpha), \quad (4)$$

$$\ln k = \ln A - E/RT. \quad (5)$$

Here α is the sample weight fraction that decomposed in time t; $d\alpha/dt$, reaction rate; and $f(\alpha)$, a mathematical expression for α.

Joint solution of Eqs. (4) and (5) yields expression (6).

$$\ln\left(\frac{d\alpha/dt}{f(\alpha)}\right) = \ln A - E/RT. \quad (6)$$

The sample weight fraction α can be calculated by Eq. (7).

$$\alpha = \frac{\omega_i - \omega_t}{\omega_i - \omega_f}. \quad (7)$$

Here ω_i is the initial sample weight; ω_t, sample weight at a certain instant of time or at temperature t; and ω_f, final sample weight.

The differentiation of Eq. (7) gives expression (8).

$$\frac{d\alpha}{dt} = \frac{d\omega_t/dt}{\omega_i - \omega_f}. \quad (8)$$

The function $(d\omega_t/dt)$ can be obtained directly from DTG data, and the reaction rate can be calculated by Eq. (8). The resulting value of $d\alpha/dt$ is substituted in Eq. (6), and the plot of

$$\ln\left(\frac{d\alpha/dt}{f(\alpha)}\right) - 1/T$$

is constructed. This plot is completely analogous to the Arrhenius plot. When substituting a mathematical expression of function $f(\alpha)$ from [20, 21], it is necessary to achieve a straight line. Then the chosen value of the function $f(\alpha)$ will reflect the reaction mechanism; the slope of this line, the activation energy; and a segment cut off on the y-axis, the preexponential factor.

We also used a simple procedure for calculating the apparent activation energy from the DTG data [9]. The procedure was based on the Arrhenius equation in the logarithmic form (5). Plots of the deviation of the DTG curve from the baseline were constructed in the coordinates $\log \Delta h - 1/T$. The value of Δh was measured directly from the DTG curve. The activation energy is proportional to the slope of the resulting linear dependence $\log \Delta h - 1/T$.

As a reference substance for estimating the correctness of kinetic parameters to be determined we used $KMnO_4$ mixed with Al_2O_3. The calculated kinetic characteristics of $KMnO_4$ thermal decomposition and the published data are given below.

Sample	E_a, kJ mol^{-1}	
$KMnO_4$–Al_2O_3, 1 : 1	140.52 (r^2 0.961)	[11]
	140.74 (r^2 0.995)	[12]
	141.59 (r^2 0.967)	[13]
	135.43–144.21	[11]

ACKNOWLEDGMENTS

This study was financially supported by Presidium of the Russian Academy of Sciences (Program of basic research "Directed Synthesis of Inorganic Substances with Preset Properties and Development of Functional Materials on Their Basis," no. 8P) and by the Foundation for the Support of Domestic Science.

REFERENCES

1. Solov'ev, A.B. and Timashev, S.F., *Usp. Khim.,* 2003, vol. 72, no. 11, p. 1095.
2. Ding, H., Erokhin, V., Ram, M.K., Paddeu, S., Valkova, L., and Nicolini, C., *Thin Solid Films,* 2000, vol. 379, p. 279.
3. Lee, Y.-L., Hsiao, C.-Y., Chang, C.-H., and Yang, Y.-M., *Sens. Actuators B,* 2003, vol. 94, p. 169.
4. Ottaviano, L., Lozzi, L., Phani, A.R., Ciattoni, A., Santucci, S., and Di Nardo, S., *Appl. Surf. Sci.,* 1998, vol. 136, p. 81.
5. Lebedeva, N.Sh., Pavlycheva, N.A., Vyugin, A.I., Kulinich, V.P., Shaposhnikov, G.P., and Parfenyuk, E.V., *J. Therm. Anal. Calorim.,* 2005, vol. 81, p. 451.
6. Mochalova, N.L., Snegireva, F.P., Maizlish, V.E., and Shaposhnikov, G.P., *Izv. Vyssh. Uchebn. Zaved., Khim. Khim. Tekhnol.,* 1988, vol. 31, no. 12, p. 116.
7. Allan, J.R., Paton, A.D., Turvey, K., Gerrard, D.L., and Holy, S., *Thermochim. Acta,* 1989, vol. 143, p. 67.
8. Berezin, B.D. and Enikolopyan, N.S., *Metalloporfiriny* (Metalloporphyrins), Moscow: Nauka, 1988.
9. Zatsepin, A.F., Fotnev, A.A., and Dmitriev, I.A., *Zh. Neorg. Khim.,* 1973, vol. 18, no. 11, p. 2883.
10. Lebedeva, N.S., Antina, E.V., and V'yugin, A.I., *Zh. Fiz. Khim.,* 1999, vol. 73, no. 6, p. 1051.
11. Rosca, I. and Foca, N., *J. Therm. Anal. Calorim.,* 1999, vol. 56, p. 401.
12. Segal, E., *Festkorper-Chemie,* Boldyrev, V.V., and Meyer, K., Eds., Leipzig: Grundstoffindustrie, 1973, p. 404.
13. Wu, D., Xu, G., Qu, S., Xue, R., Gu, C., and Zhang F., *Thermochim. Acta,* 1989, vol. 154, p. 233.
14. Dneprovskii, A.S. and Temnikova, T.I., *Teoreticheskie osnovy organicheskoi khimii* (Theoretical Foundations of Organic Chemistry), Leningrad: Khimiya, 1979.
15. Paul, K.G. and Holberg, C., *Chem. Scripta,* 1985, vol. 25, p. 177.
16. Antina, A.E., Lebedeva, N.S., V'yugin, A.I., and Stroikova, I.K., *Zh. Fiz. Khim.,* 1998, vol. 72, no. 4, p. 721.
17. Askarov, K.A., Berezin, B.D., Evstigneeva, R.P., et al., *Porfiriny: struktura, svoistva, sintez* (Porphyrins: Structure, Properties, Synthesis), Moscow: Nauka, 1985.
18. Berezin, B.D., *Koordinatsionnye soedineniya porfirinov i ftalotsianina* (Coordination Compounds of Porphyrins and Phthalocyanine), Moscow: Nauka, 1976.
19. Lebedeva, N.Sh., Yakubov, S.P., Kinchin, A.N., and V'yugin, A.I., *Zh. Fiz. Khim.,* 2005, vol. 79, no. 5, p. 958.
20. Santani, M., Dollimore, D., and Alexander, K.S., *Thermochim. Acta,* 2002, vols. 392–393, p. 135.
21. Wendlandt, W.W., *Thermal Methods of Analysis,* New York: Wiley, 1974, 2nd ed.